

Microstructural and mechanical characterization of TP-650 titanium matrix composites

Weidong Song^{1,*}, Jianguo Ning¹, Fang Jiang¹ and Xiaonan Mao²

¹State Key Laboratory of Explosion Science and Technology, Beijing Institute of Technology, Beijing 100081, P.R.China

² Northwest Institute for Non-ferrous Metal Research, Xi'an 710016, P.R.China

Abstract

Quasi-static and dynamic tensile tests were performed at room and high temperature to investigate the microstructural and mechanical characterization of TP-650 titanium matrix composites produced by pre-treatment melt process (PTMP). It was shown that both the matrix and the composite demonstrate some strain-rate sensitivity and the mechanical behavior of the composite material was influenced by the addition of the TiC particle (TiCp). The fracture surfaces for both the matrix and the composite were explored using a scanning electron microscope (SEM) showing that the failure of the composite was controlled by the brittle fracture of TiCp followed by the ductile fracture of the titanium matrix.

Keywords: titanium alloys, tensile test, fracture behavior, SEM

1 Introduction

Nowadays, much attention has been paid to titanium alloys due to their higher stiffness-to-weight ratio, strength-to-weight and good high-temperature properties. Because of these special characteristics, these alloys have been used widely in aerospace, automotive and gas-turbine industries [13]. With the never-ending quest for lighter and stronger material in above fields, there is considerably interest in the development of titanium matrix composites (TMCs) for high-temperature environments [2, 11].

There are several processing technologies adopted in industrial production, such as cold and hot isostatic pressing (CHIP), solidification processing, exothermic processing, and so on [13]. There are considerable literatures available about the mechanical properties of titanium alloys producing by different methods under quasi-static loading [3, 4, 6–10, 12, 16, 18–20]. However, the elongation of these composites produced by different methods is just about 2% at room temperature, which is too low for engineering applications. Northwest Institute for Non-ferrous Metal Research has developed a Pre-treatment melt process (PTMP) to manufacture TiC particulate-reinforced composites TP-650 [14, 15, 21]. PTMP includes three stages: firstly, the titanium alloy

*Corresp. author email: swdgh@bit.edu.cn

and reinforcement are mixed intensively; secondly, the mixture was pre-sintered and pressed with titanium sponge to create consumable electrode; finally, arc melting was adopted to prepare titanium matrix composites. Antonio et al. [5] investigated the micro-structural and mechanical characterization of a TiAl4V/TiC/10p composite processed by the BE-CHIP method and found that the distribution of the reinforcement had strong influences on the mechanical properties of the composite material, but the elongation at 375⁰C is only 1.41%. Segurado et al. [17] reported that the presence of particle clustering led to a large reduction in the flow stress of the composite because of the rapid fracture of the reinforcement. Abkowitz and Weihrauch [1] studied the mechanical behavior of a Ti6Al4V/TiC/10p from room temperature to 650⁰C and observed a dramatic increase in stiffness of the composite. Though they reported the fracture toughness of the composite was about 28MPam^{1/2}, this composite had limited room temperature ductility. While there are still many areas which lack understanding, the main focus of recent work is to achieve optimum properties at high temperature in these composites.

In order to provide technical support for aircraft engine and some heat resistant parts for automobile industries, the present paper focuses on the micro-structural and mechanical properties of TP-650 titanium matrix composites under quasi-static and dynamic loading at room and high temperature.

2 Experimental procedures

The material used in the present study was all TP-650 titanium matrix composite reinforced with 10%vol. of TiCp manufactured by Northwest Institute for Non-ferrous Metal Research. The average particle diameter of the reinforcement was about 5 μ m and the constituents of the composite were Ti-4.0~6.0Al-0.4~0.8Mo-0.3~0.6Si-2.0~3.0Sn-3.5~4.5Zr+nTiC. The reinforced particle (TiCp) dispersed homogeneously in the matrix. The interfacial reaction layers between the particle and the matrix were stable and the reaction zone width was less than 3 μ m. The TP-650 composite has no brittle phase and present good plasticity at room temperature and high temperature. The composite can keep high tensile strength at the temperature of 650⁰C. The composites were fabricated to the 20mm diameter bars. Then the diameter of the composite was forged into 13mm by rotary swaging at the temperature of 1000⁰C. The heat treatment for TP-650 composites was carried out according to the following procedures: Heat preservation at 800⁰C for 1h, AC. After the heat treatment, the bars were fabricated to the tensile specimen.

Mechanical behaviors of TP-650 were explored through tensile tests at different temperatures and different strain rates. The micro-structural features of the TP-650 composite and the matrix were investigated by using scanning electron microscopy (SEM).

Table 1 and Table 2 show the mechanical properties of TiC, titanium alloy matrix and TP-650 composites.

Table 1: The mechanical properties of TiC and titanium alloy matrix

	TiC particle	titanium alloy matrix
Density $\rho/g/cm^3$	4.43	4.51
Youngs modulus E / GPa	460	118
Shear modulus G/GPa	193	43
Poisson's ratio ν	0.188	0.35

Table 2: The mechanical properties of TP-650 composite

	Room temperature	650°C	700°C
Tensile strength σ_b/MPa	1340	680	
Yield strength σ_s/MPa	1270	590	580
Yield strength $\sigma_{0.2}/MPa$	1280	560	479
Elongation δ	8~5%	9.5%	
Youngs modulus E/GPa	136~141		
Area reduction ψ		35%	

2.1 Room temperature tensile tests

Room temperature tensile tests have been conducted in 4 specimens using MTS810 servocontrolled fatigue testing machine at a nominal applied strain rate of $10^{-4} - 10^{-3}s^{-1}$. The four specimens were machined respectively from the titanium alloy matrix and the TP-650 composite bars (20mm and 13mm diameter bars) via linear cutting. The displacement rates of MTS810 were 0.15mm/min and 1.5mm/min, respectively. The specimens were all round (5mm diameter and 30mm gauge length) shown in Fig. 1(a).

2.2 Dynamic tensile tests

Dynamic tensile tests have been performed for the matrix and the composite in 6 specimens using SHTB at different strain rates at room temperature. Fig.2 shows the schematic of SHTB used dynamic tensile tests. The experimental set-up is consists of loading system, impactor, input bar and output bar. The impactor was driven by a flywheel with a diameter of 1.4m and its linear velocity can reach 100m/s.

The specimen was connect with the input bar and output bar by glue with a high strength

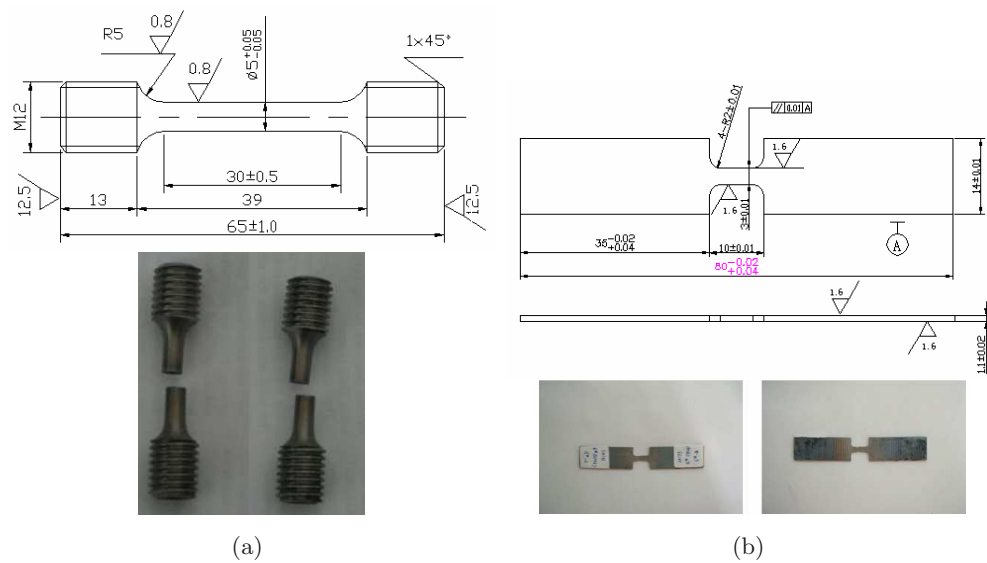


Figure 1: Schematic and photograph of the quasi-static (a) and the dynamic (b) tensile test specimen

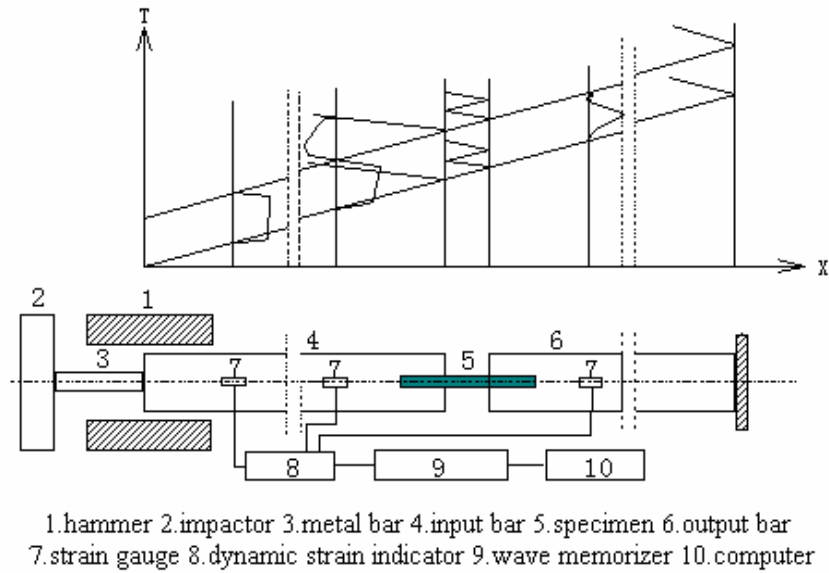


Figure 2: Schematic of experimental set-up

to avoid the wave dispersion caused by the thread grooves of the specimen. The specimen was dumbbell-shape and the schematic of the specimen was shown in Fig.1(b). Three strain rates, 200s^{-1} , 500s^{-1} and 1000s^{-1} , were adopted in the tests. For each strain rate, more than three tests were conducted for each strain rate and the average values were obtained according to the experimental results with good repeatability.

The signals of incident wave ε_i , reflected wave ε_r and transmission wave ε_t were magnified by the dynamic strain indicator through three groups of strain gauges attached to the input bar and the output bar. Then the signals were recorded by TCL wave memorizer. The responding time of the strain gauges is $2 \times 10^{-7}\text{s}$ and the resolution is 10^{-6}

If the input bar and the output bar are made of the same material and have the same cross-section area, the strain, the strain rate and the stress can be calculated by the following formula:

$$\varepsilon(t) = \frac{C_0}{L_0} \int_0^t [\varepsilon_i(\tau) - \varepsilon_r(\tau) - \varepsilon_t(\tau)] d\tau \tag{1}$$

$$\dot{\varepsilon}(t) = \frac{C_0}{L_0} [\varepsilon_i(t) - \varepsilon_r(t) - \varepsilon_t(t)] \tag{2}$$

$$\sigma(t) = \frac{EA}{2A_0} [\varepsilon_i(t) + \varepsilon_r(t) + \varepsilon_t(t)] \tag{3}$$

where E , A and C_0 are the Young's modulus, cross-section area, elastic longitudinal wave velocity of the input bar and the output bar, respectively. The incident wave ε_i and reflected wave ε_r are measured by the strain gauges on the input bar and the transmission wave ε_t is measured by the strain gauges on the output bar.

2.3 High temperature tensile tests

High temperature tensile tests were performed from room temperature to 1020°C for 10 specimens using Instron1185 testing machine at a nominal applied strain rate of $1.2 \times 10^{-3}\text{s}^{-1}$. The specimens were all round (5mm diameter and 30mm gauge length) shown in Fig. 1(a). The effect of temperature on the tensile strength was studied.

3 Experimental results and analysis

Table 3 demonstrates the loading parameters, the tensile strength, the yield strength and Young's modulus for the matrix and the composite.

As shown in Table.3, the tensile strength, the yield strength and the Young's modulus for TP-650 increased markedly with the presence of TiCp. Reasons for the increase of the tensile strength and the yield strength can be explained that the matrix and the reinforcement with high strength and high hardness will experience different deformations under tensile loading.

Table 3: The mechanical properties of the matrix and the composite

No.		$\dot{\epsilon}/s^{-1}$	σ_b/ MPa	σ_s / MPa	E / GPa
1	matrix	1×10^{-4}	1050	980	115
2	matrix	1×10^{-3}	1075	1050	116
3	TP-650	1×10^{-4}	1170	1100	132
4	TP-650	1×10^{-3}	1210	1170	131

Deformation appears first in the matrix with high ductility, while the reinforcement undergoes small or no deformation, which leads to a deformation misfit at the reinforcement-matrix interface causing a stress concentration at the interface. The stress concentration on the interface will lead to the formation of the non-uniform deformation dislocation source. The stress concentration on the interface will be set free by releasing the dislocation loop. At the same time, the dislocation density will increase in the matrix. Then, the high density dislocation will twist and react with each other, which eventually leads to the formation of dislocation cells causing an increase of strength in the matrix.

Fig.3 shows the stress-strain curves for the matrix and the composite under two quasi-static strain rates, respectively. The quasi-static strain rates are $10^{-3}s^{-1}$ and $10^{-4}s^{-1}$.

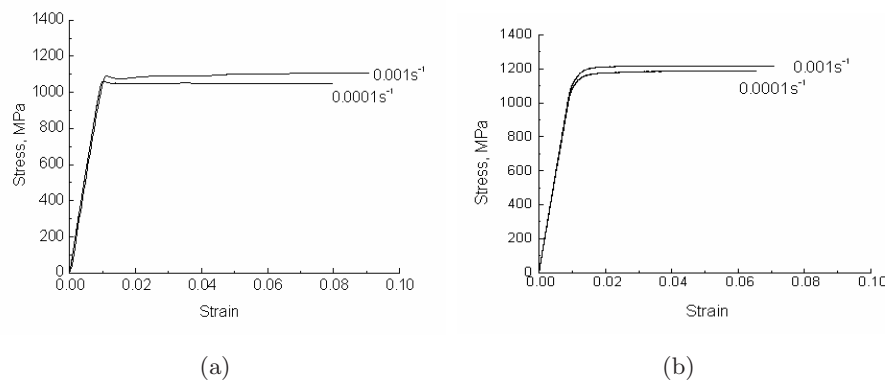


Figure 3: Quasi-static tensile stress-strain behavior of the matrix (a) and the composite TP-650 (b)

From these figures, it can be seen that both the matrix and the TP-650 composite show no obvious nonlinear phenomena under the two quasi-static strain rates prior to peak stress. When the stress reaches the yield point, the nonlinearity will appear. There is almost no hardening effect in the tensile process until the failure of the matrix and the composite. Meanwhile, both the matrix and the composite demonstrate some strain-rate sensitivity, which means that the yield strength and the tensile strength for both material increase with the increasing of strain rate.

The lower rupture strain (7%) of TP-650 composite compared to the titanium alloy matrix (8.6%) was mainly ascribed to the addition of TiCp. There are two reasons for the deterioration in ductility: the possible defects generated during the fabrication processes, such as voids and micro-cracks, and the early debonding between the reinforcement and the matrix. Due to the stiffer nature of TiCp, the composite has a higher Young's modulus than that of the matrix.

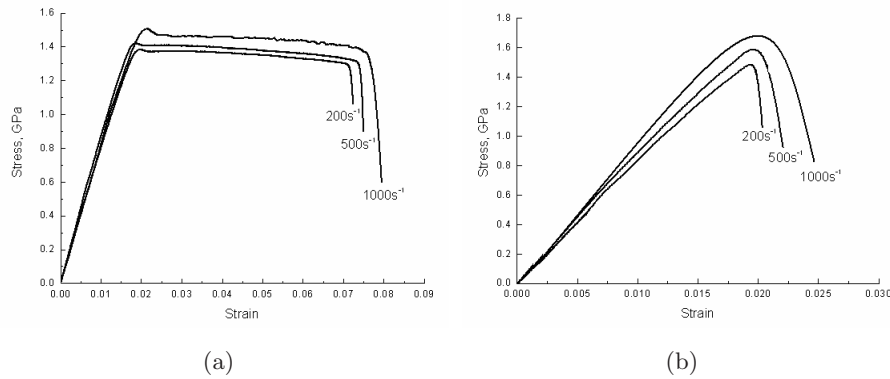


Figure 4: Dynamic tensile stress-strain behavior of the matrix (a) and the composite TP-650 (b)

Fig.4 shows the stress-strain curves of the matrix and the composite under the strain rates of $200s^{-1}$, $500s^{-1}$ and $1000 s^{-1}$. These figures reveal that the titanium alloy matrix and the TP-650 composite are strain rate dependent and both of them demonstrate obvious softening phenomena under dynamic loading. Reasons for the softening phenomena can be explained that with the increase of strain rate, high density dislocation and dislocation substructures appeared in the matrix around the particle, especially in the angle of the matrix. High stress concentration caused by the high density dislocation led to the interface debonding, matrix cracking and particulate fracture. The softening of the composite was chiefly attributed to the damages caused by the stress concentration.

With the increasing of strain rate, the stress peak of the matrix increases from 1.37GPa to 1.5GPa and for the composite, the stress peak increases from 1.5GPa to 1.7GPa.

Fig.5 presents the tensile strength of TP-650 at different temperatures. As shown in Fig.5, the effect of temperature has large influences on the tensile strength. It is important to note that the tensile strength drops sharply from 1350MPa (at room temperature) to 1020MPa (at 300⁰C). Then the reduction in the tensile strength slows down from 300⁰C to 600⁰C. When the temperature is higher than 600⁰C, the TP-650 composite will show large reductions in the tensile strength. The plastic deformation was mainly caused by the slipping of the dislocation. When the dislocation on the slipping face moved to a certain extent, the movement of the dislocation was stopped by the slip resistance and caused plastic deformations.

The high temperature behavior was explained that with the addition of TiCp the density and the multiplication rate of dislocations increases at high temperature, therefore resulting in an

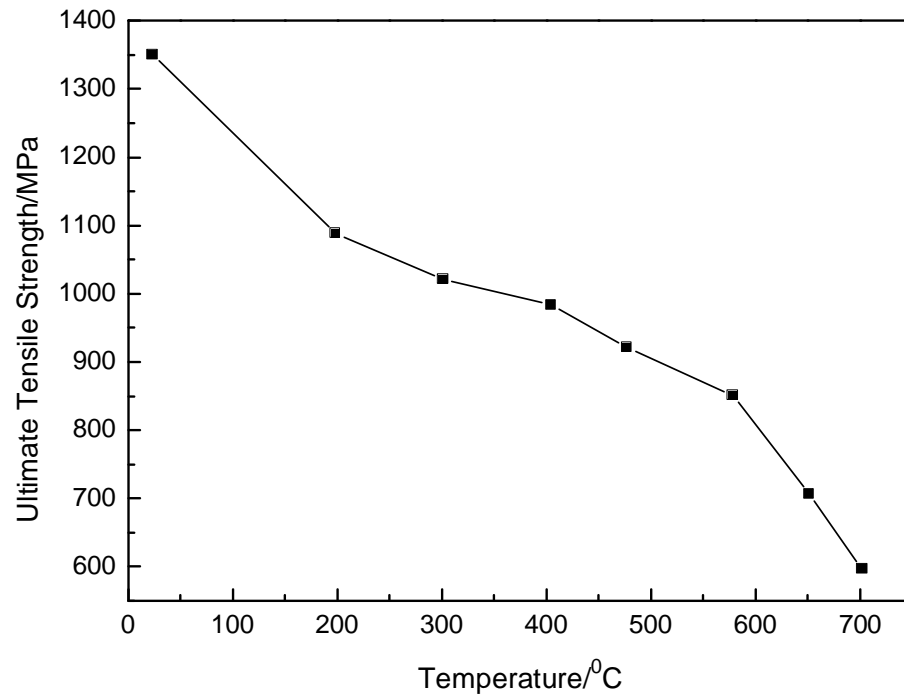


Figure 5: The tensile strength of TP-650 at different temperatures [1]

increase in the dislocation resistance and improve the high temperature mechanical properties of TP-650.

4 Microstructural characteristics and analysis

Microstructures and fracture behavior of the matrix and the composite were investigated using scanning electron microscopy (SEM).



Figure 6: Original microstructures of the composite TP-650 and the matrix [22]

Fig.6 shows the particle shape and the distribution of TiC reinforcement in the TP-650 composite. It can be seen that the TiCp is spherical and the interfaces between the reinforcement

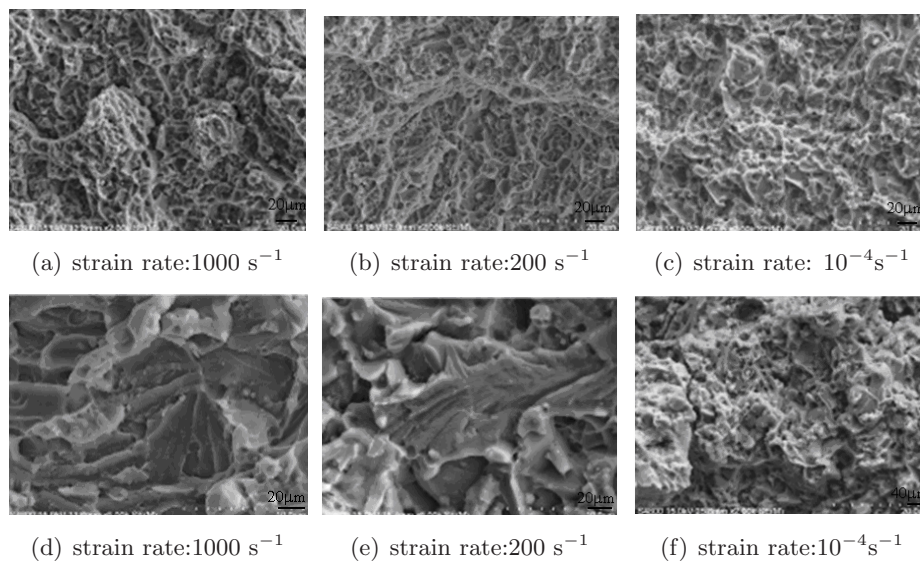


Figure 7: Quasi-static and dynamic tensile fracture surfaces of the matrix (a-c) and the composite (d-f)

and the matrix are clear and smooth, revealing that there is a metallurgical bonding annulus around the particle. The annulus is the degradation conversion zone of TiC in the matrix. The near-net shape solid phase is also found in the matrix. The intergranular precipitation for both the annulus and the near-net shape solid phase greatly improves the high temperature mechanical properties of the composite.

SEM micrographs in Fig.7 present the fractograph of the composite TP-650 and the titanium alloy matrix. The fracture surface analysis performed in the SEM has indicated ductile fracture of the matrix under dynamic loading (see Fig.7(a)-Fig.7(c)). With the increase of strain rate, the dimple size, the dimple depth and the solute particles decrease to a certain extent. The instantaneous local energy and the micro-voids increase rapidly with the increase of the strain rate. Meanwhile the cracking initiation and propagation correspondingly increase, causing the fracture of many solute particles in the dimples.

Fig.7(c) shows a high amount of dimples in the fracture surfaces and ductile fracture of the matrix. From Fig.7(f), it can be seen that TiCp is the main reason for the crack initiation and brittle fracture of the composite accompanying by secondary crack.

Under high strain rates, the cross section of the composite presents herringbone patterns. There are some crystal facets and almost no tear ridge is observed at higher magnification, but some secondary cleavages. The herringbone pattern becomes more evident as the strain rate increases.

Fig.7(d)-Fig.7(f) depict the fracture surfaces of TP-650 composite under quasi-static and dynamic tensile loading. It can be concluded that the dimples are small in the fracture surfaces

under quasi-static and dynamic loading and the composite shows no obvious ductile fracture. There is a high amount of tear ridges and some river markings in local areas, presenting complicated fracture characteristics. The dimple sizes of the dynamic fracture surfaces are larger than that of the quasi-static fracture surfaces and the deformation bands are wider. There is almost no particle fracture found in TP-650 composite from initial deformation to final failure, while there has been found an amount of debonding between the particle and the matrix.

5 Conclusions

The room and high temperature mechanical behavior under quasi-static and dynamic loading as well as the metallurgical characteristics of PTMP processed TP-650 were investigated. The following conclusions can be obtained:

- (1) The elongation at room temperature and the tensile strength at 650⁰C of TP-650 are over 5% and 650MPa with the introduction of TiCp.
- (2) The titanium alloy matrix and the TP-650 composite are strain rate dependent and both of them demonstrate softening phenomena under dynamic loading.
- (3) The failure of the composite was controlled by the brittle fracture of TiCp followed by the ductile fracture of the titanium matrix.
- (4) The deformation misfit on the reinforcement-matrix interface results in the initiation of dislocation loop causing the increase of the dislocation density in the matrix, which contributes to the strength of the matrix.

Acknowledgements

This study has been supported by the National Nature Science Foundation of China (10625208, 10602008) and Northwest Institute for Non-ferrous Metal Research.

References

- [1] S. Abkowitz and P. Weihrauch. Trimming the cost of MMCs. *Adv. Mater. Proce.*, 136:31–4, 1989.
- [2] C. Badini, G. Ubertalli, and D. Puppò. High temperature behavior of a Ti-6Al-4V/TiCp composite processed by BE-CIP-HIP method. *J. Mater. Sci.*, 35:3903–12, 2000.
- [3] C.J. Boehlert, C.J. Cowen, and S.Tamirisakandala. et al. In situ scanning electron microscopy observations of tensile deformation in a boron-modified Ti-6Al-4V alloy. *Scripta. Mater.*, 55:465–68, 2006.

-
- [4] S.J. Connell and F.W. Zok. Measurement of the cyclic bridging law in a titanium matrix composite and its application to simulating crack growth. *Acta Mater.*, 45:5203–11, 1997.
- [5] Antonio A.M. da Silva, Jorge F. dos Santos, and Telmo R. Strohaecher. Microstructural and mechanical characteristic of a Ti6Al4V/TiC/10p composite processed by the BE-CHIP method. *Comp. Sci. Tech.*, 65:1749–55, 2005.
- [6] T.J.A. Doel and P. Bowen. Tensile properties of particulate-reinforced metal matrix composites. *Comp. A*, 27:655–65, 1996.
- [7] Q. Fang, P.S. Sidky, and G.M. Hocking. Cracking behaviours and stresses release in titanium matrix composites. *Mat.Sci.Eng A.*, 288:142–47, 2000.
- [8] C.R. Feng, D.J. Michel, and C.R. Crowe. The formation of Ti3Al within TiAl during the deformation of XDTM titanium aluminide. *Scripta. Metal.*, 23:241–46, 1989.
- [9] D. Hu, T. P. Johnson, and M. H. Loretto. Titanium precipitation in substoichiometric TiC particles. *Scripta Mater.*, 30:1015–20, 1994.
- [10] D.G. Konitzer, M.H. Loretto, and Mater. Interfacial interactions in titanium-based metal matrix composites. *Sci. Eng.*, 107A:217–23, 1989.
- [11] G. Liu, D. Zhu, and J-K. Shang. Temperature dependence of fracture toughness in TiC-particle reinforced Ti-6Al-4V matrix composite. *Scripta Metall Mater.*, 28:729–32, 1993.
- [12] M.H. Loretto and D.G. Konitzer. The effect of matrix reinforcement reaction on fracture in Ti-6Al-4V-base composites. *Metall Mater Trans.*, 21:1579–87, 1990.
- [13] W.J. Lv and D. Zhang. *Fabrication, microstructure and mechanical properties of in situ synthesized titanium matrix composites*. Higher education press, Beijing, 2005.
- [14] X.N. Mao, L. Zhou, and Q.P Zeng. et al. Deformation fracture of titanium matrix composites reinforced by TiC particles. *Rare. Metal. Mater. Eng.*, 29:218–20, 2000.
- [15] X.N. Mao, L. Zhou, and Y.G. Zhou. et al. Characteristic of principle properties and microstructure of TP-650 particles reinforced titanium matrix composites. *Rare. Metal. Mater. Eng.*, 33:620–23, 2004.
- [16] S. Ranganath. A review on particulate-reinforced titanium matrix composites. *J. Mater. Sci.*, 32:1–16, 1997.
- [17] J. Sequ rado, C. Gonzalez, and J. Llorca. A numerical investigation of the effect of particle clustering on the mechanical properties of composites. *Acta Mater.*, 51:2355–69, 2003.
- [18] J. Subrahmanyam and M. Vijayakumar. Self-propagating high-temperature synthesis. *J. Mater. Sci.*, 27:6249–73, 1992.
- [19] S.C. Tjong and Z.Y. Ma. Microstructural and mechanical characteristics of in situ metal matrix composites. *Mater. Sci. Eng*, 29:49–113, 2000.
- [20] Y.L. Xi, D.L. Chai, and W.X. Zhang. et al. Titanium alloy reinforced magnesium matrix composite with improved mechanical properties. *Scripta. Mater.*, 54:19–23, 2006.
- [21] Y.J. Zhang, Q.P. Zeng, and X.N. Mao. et al. Strength estimation of a Ti alloy matrix composite reinforced by TiC particles. *Rare. Metal. Mater. Eng.*, 28:265–68, 1999.

